

Polyelectrolyte Behavior of an Interpolyelectrolyte Complex Formed in Aqueous Solution of a Charged Dendrimer and Sodium Poly(L-glutamate)

Dietrich Leisner and Toyoko Imae*

Research Center for Materials Science, Nagoya University, Chikusa, Nagoya 464-8602, Japan

Received: February 17, 2003; In Final Form: August 9, 2003

The binding of the protonated fourth generation poly(amido amine) dendrimer as a guest polyelectrolyte (GPE) to the anionic homopolyelectrolyte poly(L-glutamic acid) sodium salt as a host polyelectrolyte (HPE) has been investigated by potentiometric and turbidimetric titration in aqueous 0.25 M NaCl solutions. The polyelectrolyte behaviors of interpolyelectrolyte complex (IPEC)-forming mixtures were compared with those of hypothetically noninteracting individual polyelectrolytes (PEs) at different stoichiometric ratios, Φ , of GPE to HPE. From the overall degree of protonation, β , at a given pH and Φ , the degree of conversion, $\Theta(\text{pH})$, of oppositely charged groups to ion pairs with released counterions has been calculated, as well as the thermodynamic dissociation constant, K_D , of an ion pair in the IPEC. A high cooperativity of the binding of the ammonium groups of the GPE to the HPE is concluded from the strong linear increase in the $\text{p}K_D$ with Θ . As soon as the GPE becomes partly charged below pH 11, both Θ and the turbidity, which are proportional to the molecular weight, increase linearly with the decreasing pH, showing that the initial increase in Θ is due to an increased number of bound GPEs. From the increase in Θ to well above 0.5, it is likely that the linear HPE penetrates partly into the interior shells of the dendrimer GPE.

Introduction

Interpolyelectrolyte complex (IPEC) formation between oppositely charged polyelectrolytes (PEs) in aqueous solution originates predominantly from the charge attraction correlation of charged groups in the polyions, which delocalizes the replaced small counterions and thus increases the entropy.^{1–3} However, as macroion ligand exchange reactions⁴ have shown, the chemical nature of the ion pair as well as unspecific (e.g., hydrophobic) interactions and steric constraints for the coupling of semiflexible or stiff PEs play important roles. The latter become more evident when the electrostatic attraction is limited by low surface potentials of the interacting PEs. Most systematic studies on the qualitative influence of these factors have been performed on IPECs between linear PEs.⁵ The interaction between a linear PE and spherical⁶ or cylindrical⁷ compact micelles has also been studied in detail, showing critical values of the charge density required for the onset of PEC formation which do not depend on the colloid geometry. However, the critical charge density decreases with increasing charge density of the encounter⁸ and increases with screening either by the ionic strength^{9,10} or by the solvent (increased hydrophilicity of either of the interacting colloids), as has been shown in studies with micelles on modified HPEs.¹¹ Studies with different proteins close to their isoelectric points¹² have shown that for interacting heteropolyelectrolytes the charge density in interacting patches is the critical parameter, but the average charge density of the colloids is not.¹³

More recently, IPEC formation with rather uniformly charged dendrimers and star polymers has been investigated in more detail, both experimentally and theoretically. In contrast to micelles that carry their charges exclusively at the periphery, even the terminal groups of flexible dendrimers are distributed

in a shell of considerable diffuseness, as has been shown by Monte Carlo simulations.^{14,15} Further ionized groups can be located exclusively in the inner shells of the dendrimer. The most effective ion pairing with a linear polyelectrolyte then requires mutual interpenetration of the different PEs. Whereas, for example, flexible PEs are able to form ion pairs with all the interior ionic sites of a G5 poly(propyleneimine) dendrimer,¹⁶ stiff double-stranded DNA is found to interact only with the periphery of that dendrimer.¹⁷ The different chemical and steric accessibilities of the different sites in the dendrimer offers a range of selectivity for the concurrent binding of different PEs and smaller guest molecules whose association constants can profit from adequate cavities in larger dendrimers.

Thus, with respect to drug delivery by dendrimers and star polymers,^{18–20} their IPEC formation with proteins, peptides, and DNA²¹ under different physiological conditions is of considerable interest. In particular, soluble IPECs in aqueous solutions containing a moderate salt are interesting, because such complexes should easily be transported in the blood.

As has been learned from the studies with IPECs between linear PEs, the formation of soluble IPECs usually requires at least one of the constituting PEs to be hydrophilic but not highly charged. Further, a stoichiometry allows for residual charge of the IPEC, and/or a sufficiently high dilution. For weak PEs and proteins (polyampholytes), the charge density on the segments or patches can usually be modified and principally controlled by the pH of the solution. Quantitative understanding of the interplay between proton dissociation and the reversible IPEC formation would be advantageous for the success of selectivity studies in the future.

In this paper, we investigate soluble IPEC formation between a linear semiflexible poly(L-glutamate) as an anionic HPE and a partially protonated and thereby positively charged poly(amido amine) dendrimer of intermediate generation, G4, as a GPE. This system was chosen to mimic the unspecific part of the

* Corresponding author. Tel: +81-52-789-5911. Fax: +81-52-789-5912. E-mail: imae@nano.chem.nagoya-u.ac.jp.

guest–host interaction of the dendrimer with a long polypeptide with a low isoelectric point (PI), i.e., to allow for a dipole–dipole and hydrogen-bonding interaction between the amide groups in the HPE backbone and the 124 amino groups in the dendrimer branches, in addition to the ion pairing of the ammonium and carboxylate groups. We examine the dependence of the average binding constant on the dendrimer (GPE) charge from the polyelectrolyte behaviors of the individual PEs and of the interacting mixtures.

The polyelectrolyte behaviors of both the poly(L-glutamic acid) (PGA)²² and some poly(amido amine) (PAMAM) dendrimers^{23–25} in aqueous solutions of various ionic strengths have been reported in the literature. In the case of PGA, the behavior was fitted by successful Monte Carlo simulations,²⁶ which take into account the transition from the α -helical conformation at low effective charge density to the extended coil conformation at higher charge density or less screening. Unfortunately, no data were available for 0.25 M NaCl aqueous solution at 25 °C, the solvent condition used throughout this study.

In the course of this paper, therefore, we first analyze and describe the polyelectrolyte behaviors of the two individual polyelectrolytes under these solvent conditions. Subsequently, the interaction and IPEC formation between the weak polyelectrolytes are analyzed in terms of an average dissociation constant for an ion pair, as functions of their pH-dependent ionization and of the stoichiometric ratio GPE/HPE, at a constant concentration of the HPE. The critical charge density on the dendrimer for the onset of IPEC formation and that for phase separation (coacervation) are investigated by turbidimetric titrations, and the binding observed from the initial turbidity increase is compared with the extent of ion-pair formation estimated from the change in the overall ionization behavior.

Theory

Dissociation Equilibrium of a Homopolyelectrolyte. The dissociation of a homopolyelectrolyte $[-(\text{AH})^z-]_n$ in aqueous solution with formal charge z per protonated monomer and degree of polymerization n can be described by the reaction scheme



where the distribution of the $m = \alpha n$ deprotonated out of n ionizable groups is rather statistical than blockwise, to satisfy major entropy and screening between ionic sites. The molar free energy of the reaction is $\Delta G(\alpha) = -RT \ln K_a(\alpha)$, where $R = k_B N_A$ is the molar gas constant (with k_B Boltzmann constant and N_A the Avogadro constant) and T is the absolute temperature. The apparent dissociation constant $K_a(\alpha)$ is related to the experimentally accessible pH(α) by the Hasselbalch relationship²⁷

$$\text{p}K_a(\alpha) \equiv -\log_{10}[K_a(\alpha)] = \text{pH}(\alpha) - \log_{10}[\alpha/(1 - \alpha)] \quad (2)$$

The degree of deprotonation α or the corresponding degree of protonation, $\beta \equiv 1 - \alpha$, can be obtained from a proton mass balance with the initial numbers, $n_0(\text{AH}^z)$ and $n_0(\text{A}^{z-1})$, of equivalents of the acidic and basic functional groups, and those of added titrants HCl and NaOH, $n_0(\text{HCl})$ and $n_0(\text{NaOH})$, in the total volume V :

$$\alpha = \frac{n_0(\text{AH}^z) + n_0(\text{HCl}) - VC(\text{H}^+) - n_0(\text{NaOH}) + VC(\text{OH}^-)}{n_0(\text{AH}^z) + n_0(\text{A}^{z-1})} \quad (3)$$

pH(α) indicates the equilibrium concentrations $C(\text{H}^+)/[\text{M}] = 10^{-\text{pH}}/\gamma_{\pm}$ and $C(\text{OH}^-)/[\text{M}] = 10^{-14+\text{pH}}/\gamma_{\pm}$ of solvated protons and hydroxide ions, respectively, where the activity coefficient γ_{\pm} is approximated by the Davies formula,²⁸ which is a simplification of the more general extended Debye–Hückel formula²⁹ and reads for aqueous solutions up to moderate ionic strength I at 25 °C:

$$\log_{10}(\gamma_{\pm}) \cong -0.5[\sqrt{I}/(1 + \sqrt{I}) - 0.2I] \quad (4)$$

ΔG is determined not only by the intrinsic K_a^* in an (hypothetically) electroneutral colloid but also by the extra work $\Delta G_{\text{el}} = F\psi_0(\alpha)$ to generate a more asymmetric charge distribution, where $F = eN_A$ is the Faraday constant, e is the elementary charge, and ψ_0 is the surface potential at the periphery of the ionic site. The latter is thus obtained from the deviation $\Delta \text{p}K_a \equiv \text{p}K_a(\alpha) - \text{p}K_a^*$ of the apparent $\text{p}K_a$ from the intrinsic one, $\text{p}K_a^*$, as

$$\psi_0(\alpha) = \ln(10) \cdot (k_B T/e) \cdot \Delta \text{p}K_a \quad (5)$$

In spherical geometry (e.g., for a dendrimer of high generation), one has a uniform charge density σ_{GC} at a radius r corresponding to the outer Helmholtz plane of a colloid. It can be obtained with the Gouy–Chapman relation from the electrostatic surface potential:^{8,30}

$$\sigma_{\text{GC}} = (4\pi)^{-1} \epsilon_0 \epsilon_r \cdot \psi_0 \cdot (\kappa + r^{-1}) \quad (6)$$

where ϵ_0 is the dielectric permittivity of the vacuum, ϵ_r is the relative dielectric constant in the Gouy–Chapman layer, and κ is the Debye–Hückel parameter,

$$\kappa = [8\pi l_B N_A \cdot I \cdot \rho]^{1/2} \quad (7)$$

with $l_B = e^2/(4\pi\epsilon_0\epsilon_r k_B T)$ the Bjerrum length and ρ the mass density. In aqueous 0.25 M NaCl with negligible amounts of other ions at 25 °C and $\epsilon_r = 78.33$, $l_B = 0.714$ nm, and $\kappa^{-1} = 0.608$ nm, respectively.

The electrostatic field of a charged dendrimer of higher generation has been approximated by that of a sphere of constant radius R_{HS} carrying the same charge Q_{HS} ,⁸ so that

$$\sigma_{\text{HS}} = (4\pi)^{-1} \epsilon_0 \epsilon_r Q_{\text{HS}} R_{\text{HS}}^{-2} \quad (8)$$

In the counterion condensation theory (CC theory), a linear homopolyelectrolyte in the extended coil conformation is approximated by a homogeneously charged *thin* cylinder.^{31,32} With the distance b between two elemental charges along the chain and the linear charge density $\xi = l_B/b$, there exists a critical value ξ_{crit} above which counterions would condense on the chain. For $T \cdot b$ large enough to satisfy the noncondensation condition $\xi < \xi_{\text{crit}}$, the electrostatic contribution to the ion energy from each ionizable site is

$$G_{\text{el}} = -RT\xi \ln[1 - \exp(-\kappa b)] \quad (9)$$

With general polyelectrolyte theory and taking all contributions to the ion energy other than G_{el} as independent of the degree of dissociation α ,

$$\Delta pK_a(\alpha) = \frac{1}{RT \ln 10} \cdot \frac{\partial G_{el}}{\partial \alpha} \quad (10)$$

Then the CC theory gives for $\alpha \xi < \xi_{crit}$ with $C_S/C_P =$ ratio of added 1:1 salt to ionizable groups on the polymer³³ and with the assumption that the chain extension is not altered with the degree of ionization, that is $b = \alpha \cdot b_1$, where $b_1 = b(\alpha=1)$ is the distance between ionizable groups:

$$\Delta pK_a(\alpha) = -\frac{\alpha b_1/b_1}{\ln 10} \left\{ 2 \ln(u) - \frac{\kappa \alpha b_1}{u} \left[\frac{\alpha/2}{2C_S/C_P + \alpha} - 1 \right] \right\} \quad (11)$$

where $u \equiv 1 - \exp(-\kappa \alpha b_1)$.

Dissociation Equilibrium of a Heteropolyelectrolyte. A heteropolyelectrolyte with n_{pK_a} sets of chemically different but *noninteracting* sites i with their intrinsic dissociation constants given by $K_{a,i}^*$ can be treated as a homopolyelectrolyte with an ensemble-averaged intrinsic $pK_a^*(\alpha)$, which becomes a function of the overall degree of dissociation. The equilibrium dissociation in each set of sites follows the extended Hasselbalch relationship:

$$pH = pK_{a,i}^* + \Delta pK_a(\alpha) + \ln[(1 - \alpha_i)/\alpha_i] \quad (12)$$

$$\alpha_i(pH) = \frac{10^{-pK_{a,i}^* - \Delta pK_a(\alpha)}}{10^{-pK_{a,i}^* - \Delta pK_a(\alpha)} + 10^{-pH}} \quad (12a)$$

The overall degree of dissociation α is just the weighted average over the α_i :

$$\alpha(pH) = \frac{\sum_{i=1}^{n_{pK_a}} n_i \alpha_i(pH)}{\sum_{i=1}^{n_{pK_a}} n_i} \quad (13)$$

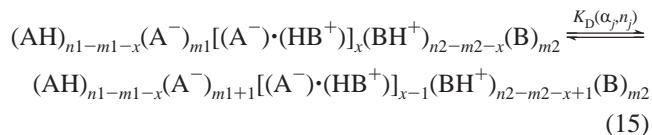
Equations 12a and 13 can be used iteratively to obtain $\alpha(pH)$ if the intrinsic $pK_{a,i}^*$ of the isolated sites, the relative composition (n_i), and the excess function $\Delta pK_a(\alpha)$ are known. The apparent pK_a may then be obtained with eq 2, and its intrinsic contribution as

$$pK_{a,i}^*(\alpha) = pK_a(\alpha) - \Delta pK_a(\alpha) \quad (14)$$

For a partially *self-interacting* polyelectrolyte, the ensemble of coupled sites would have to be represented by an ensemble of the same number of decoupled quasi-sites³⁴ with the same overall dissociation behavior, and could then be treated analogously to an ensemble of noninteracting sites.

Dissociation Equilibrium of an IPEC Forming Mixture of Polyelectrolytes. The ensemble of dissociating (quasi-) sites in a mixture of *noninteracting* polyelectrolytes can be treated similarly to that for a single heteropolyelectrolyte, except that in eq 12 different $\Delta pK_{a,i}(\alpha_i)$ values instead of a common $\Delta pK_a(\alpha)$ have to be distinguished for the sites i belonging to the ensembles of any different polyelectrolyte j . Therefore, individual α_j have to be calculated with eqs 13, in which α is replaced by α_j , from the α_i and n_i in any such ensemble j separately.

The interacting mixture of two polyelectrolytes and their IPEC can be described as an ensemble of stoichiometric ion-paired sites and noninteracting sites. The dissociation of one of x ion pairs between two oppositely charged sites A^- , BH^+ on two different weak polyelectrolytes ($j = 1, 2$), where the PE indexed by $j = 1$ carries the A^- sites, can be described by the reaction



and when $x = 0$ the polyelectrolytes separate. Equation 15 describes only the bimolecular interaction, but ion pairs can also be formed to connect many polyelectrolytes to form multimolecular and even multinuclear IPECs. The counterions localized close to the excess and unpaired (A^-) and (BH^+) functional groups are omitted. The extent of complexation is quantified¹⁶ as the degree of conversion Θ of pairs of ionizable sites to ion pairs with released monovalent counterions:

$$\Theta \equiv \frac{n_{ABH}}{\min(n_{0,A}, n_{0,B})} \quad (16)$$

where the $\min()$ function evaluates the minimum of its arguments.

It can be shown that for a mixing ratio $\Phi \equiv n_{0,B}/n_{0,A}$ the apparent ion pair dissociation constant K_D' is connected to Θ by the quadratic relationship

$$\Theta = (v/2 - \sqrt{(v/2)^2 - \Phi})/\min(1, \Phi) \quad (17)$$

where $v \equiv 1 + \Phi + K_D'/C_{0,A}$, and

$$K_D'(pH, \dots) = \frac{(C_{A,0} - C_{ABH})(C_{B,0} - C_{ABH})}{C_{ABH}} = \frac{K_D}{\alpha_A(1 - \alpha_B)} \quad (18)$$

where $K_D = C_A C_{BH}/C_{ABH}$, and α_A and α_B are the degrees of deprotonation of the fractions of PE groups not involved in the ion pairs. Conversely, the apparent dissociation constant K_D' can be obtained from the conversion ratio Θ :

$$K_D' = C_{0,A} \left[\Theta \min(1, \Phi) - 1 + \Phi \left(\frac{1}{\Theta \min(1, \Phi)} - 1 \right) \right] \quad (19)$$

Further we recognize that the degrees of association with protons, $\beta_j \equiv 1 - \alpha_j$, for the ensembles of those polyelectrolyte segments which are not involved in direct ion pairs, are

$$\beta_j = \frac{\langle n_j - m_j - x \rangle}{\langle n_j - x \rangle} \quad (20)$$

and for the ensemble of the ion paired sites in which two bases "share" a proton that should be mostly localized close to the stronger base (B), we have $\beta = 1/2$. By a weighting analogous to that in eq 13, we obtain the degree of protonation of the ensemble of all the basic sites in the mixture, $\beta \equiv 1 - \alpha$, as

$$\beta = \frac{\beta_{j=1} + \beta_{j=2} \Phi + (1 - \beta_{j=1} - \beta_{j=2}) \Theta \cdot \min(1, \Phi)}{1 + \Phi} \quad (21)$$

From the rearrangement of eq 21, Θ is obtained with the β of the mixture and the β_j of the isolated polyelectrolytes, and with their mixing ratio as

$$\Theta = \frac{\beta - \beta_{j=1} + (\beta - \beta_{j=2}) \Phi}{(1 - \beta_{j=1} - \beta_{j=2}) \cdot \min(1, \Phi)} = \frac{\alpha_{j=1} - \alpha + (\alpha_{j=2} - \alpha) \Phi}{(\alpha_{j=1} + \alpha_{j=2} - 1) \cdot \min(1, \Phi)} \quad (22)$$

In eqs 18 and 20–22 we introduced the idealization that all sites, which are not directly involved in the ion pairs, would behave as in the segments of the isolated polyelectrolytes. However, it must be expected that the absolute charge density at sites closest to those involved in the ion pairs is considerably reduced. This will enhance the proton affinity of the neutral base B and also the dissociation of the neutral acid AH. Both effects can be interpreted as a partial ion-pairing interaction which here is indeed accounted for as some extra fraction of fully interacting sites, thus as some overestimation of the Θ calculated with eq 22.

The titration curves for different Θ intersect in one point when $\beta_{j=1} + \beta_{j=2} = 1$. At a pH close to this crossover point of the titration curves, there is no different proton dissociation of the interacting or non interacting PEs and thus the degree of interaction Θ cannot be determined from a different polyelectrolyte behavior of these states.

Experimental Section

Materials. The amino-terminated Starburst poly(amido amine) dendrimer of the fourth generation with ethylenediamine core (G4-PAMAM, $M_w = 14.215k$) was supplied by Aldrich, as a 10% solution in methanol. Poly(L-glutamic acid) sodium salt (NaPGA, $M_w \cong 45k^{35}$) was supplied by Peptide Institute Inc., Lot 350922. Sodium chloride (NaCl) was of analytical grade. Water was distilled and further purified using a Millipore Milli-Q apparatus. Dilute hydrochloric acid (0.25 M HCl) and sodium hydroxide (NaOH) were prepared from Wako normal solutions.

Sample Preparation. Methanol was evaporated from the dendrimer solution in vacuo (about 0.1 mbar). NaPGA was dried in vacuo over silica gel overnight prior to use. All samples were prepared by weighing on an analytical balance, in the cases of PE mixtures from stock solutions of the individual polymers (2 g/dm³ PAMAM dendrimer, 0.2 g/dm³ NaPGA) in aqueous 0.25 M NaCl and of the solvent (aqueous 0.25 M NaCl), which had been filtered through 0.22 μm Durapore membranes (Millipore Millex GV).

Methods. All measurements were performed at 25 ± 1 °C. Hamilton syringes (50 mm³) were used for titrations. The pH was detected by combined glass electrodes (standard size: Horiba, for individual PEs; micro size: Iwaki, 4 mm o.d., for PE mixtures in $1 \times 1 \times 4$ cm quartz cuvettes). Their calibrations were carried out by three standard buffers before and after the titration. The measured pH's were corrected by a parabolic calibration function, which was validated by a blind titration with HCl. However, checking of the EMF of the microsize cell after a 4 h titration revealed a drift of the offset of up to 0.15 pH units, which was taken as linear with the number of HCl additions, whereas the slope always remained unchanged. The turbidity, $\tau = -\ln(I/I_0)$, where I/I_0 is the transmission, was measured with a Shimadzu UV 2200 spectrometer at 355 nm wavelength. In all titrations, the system was gently stirred after any addition of HCl and then allowed to equilibrate until a stable pH reading was obtained (~ 1 min, up to several minutes at some pH below 6).

Results

Polyelectrolyte Behavior of NaPGA. The proton dissociation equilibrium of NaPGA in aqueous 0.25 M NaCl was studied by potentiometric titration of a solution containing 31.9 mg of the polymer salt (0.210 mmol carboxylic side groups with equal intrinsic $pK_{a,1}^* = pK_{a,2}^*$) and 0.060 mmol NaOH in a total of 20 cm³ solution, with 0.25 N HCl. The degree of dissociation,

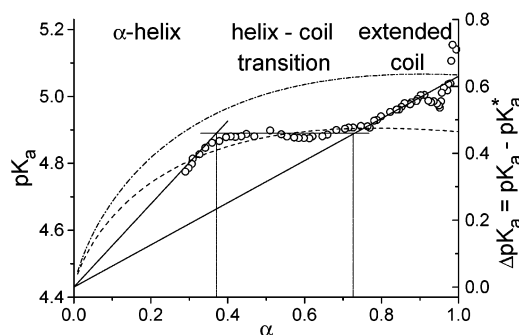


Figure 1. $pK_a(\alpha)$ obtained from extended Hasselbalch (eq 2) transformed data of the titration of 31.9 mg of NaPGA in 20 cm³ of 0.25 M aqueous NaCl with HCl. Included are linear fits to the α -helical, transition, and coiled regimes of the polyelectrolyte (solid lines), and the prediction from CC theory (eq 11), with $b_1 = 0.77$ (dashed line) and with $b_1 = 0.665$ (dashed-dotted line).

α , is determined from the calculated stoichiometry and with the fitted endpoint of the NaOH back-titration at 0.253 g HCl added. The corrected $\text{pH}(\alpha)$ readings are converted to the apparent $pK_a(\alpha)$ by the Hasselbalch relationship (eq 2) and are plotted in Figure 1. The behavior of $pK_a(\alpha)$ is well approximated by three linear regimes: two straight lines with the common intercept $pK_{a,1}^* = 4.43 \pm 0.07$ and slopes $dpK_a/d\alpha = 1.24 \pm 0.07$ (for $\alpha \leq 0.37$) and $dpK_a/d\alpha = 0.63 \pm 0.07$ (for $\alpha \geq 0.73$), respectively, and a plateau with $pK_a = 4.89 \pm 0.02$ (for $0.37 \leq \alpha \leq 0.73$). The regimes are identified as the dissociation in the α -helical conformation at low α , and as the dissociation in the more stretched extended coil conformation when α and the absolute value of the linear charge density have increased. The plateau then corresponds to the helix–coil transition, during which only the relative amounts of segments in either conformation are changed and the average charge density is maintained.

Polyelectrolyte Behavior of G4-PAMAM Dendrimer. A 0.109 g sample of G4-PAMAM dendrimer (containing 0.964 mmol basic amino groups) in 30 cm³ of aqueous 0.25 M NaCl solution was titrated with 0.25 M HCl (Figure 2a). Equation 2 and the experimental titration endpoint were used to transform the data to $pK_a(\alpha)$. The data were fitted by calculating the intrinsic contribution, $pK_{a,j}^*(\alpha)$, for a heteropolyelectrolyte with two sets, $j = 1, 2$, of ionizable groups: 64 peripheral primary amino groups with a higher $pK_{a,2}^*$ and 62 tertiary amino groups with a lower $pK_{a,1}^*$. The free $pK_{a,j}^*$ parameters varied in the first part of an iteration step in such a way that the residual function, $\Delta pK_a(\alpha)$, could be well fitted to a smooth (approximately linear) function in the second part of the iteration step. An exponential decay function was used to fit the residual curvature of $\Delta pK_a(\alpha)$, because the surface potential of the dendrimer is expected to grow more slowly than proportional to the total dendrimer charge as the electrostatic excluded volume and the dendrimer surface may increase. The fitting is shown in Figure 2b. The intrinsic $pK_{a,j}^*$ are 6.65 ± 0.07 for the 62 tertiary amino groups in the dendrimer interior, and 9.20 ± 0.05 for the 64 primary amino groups in the periphery of dendrimer. The $\Delta pK_a(\alpha)$ was fitted to

$$\Delta pK_a(\beta = 1 - \alpha) = 7.25[\exp(-\beta/7.46) - 1] \quad (23)$$

where the amplitude and decay constant are highly linearly dependent and could be fitted with an absolute precision of ± 1 . All the fitting parameters are summarized in Table 1. The $\Delta pK_a(\alpha)$ were transformed to charge densities, σ_{GC} , at the outer Helmholtz plane of the dendrimer (at radius r) using eq 6, and

TABLE 1: Properties of the Host and Guest Polyelectrolytes in 0.25 M Aqueous NaCl^a

HPE: Poly(L-glutamic acid) Sodium Salt (NaPGA)			
$M_{\text{HPE}}/\text{g}\cdot\text{mol}^{-1}$	$N_{\text{A,HPE}}$	$\text{p}K_{\text{a},i}^*$	$\Delta\text{p}K_{\text{a}}(\alpha_{\text{HPE}})$
45000 ^b	297.7	4.43 ± 0.07	$(1.24 \pm 0.07)\alpha_{\text{HPE}} \alpha_{\text{HPE}} \leq 0.37$ $(0.63 \pm 0.07)\alpha_{\text{HPE}} \alpha_{\text{HPE}} \geq 0.73$
GPE: Fourth Generation Poly(amido amine) Dendrimer (G4-PAMAM-NH ₂)			
$M_{\text{GPE}}/\text{g}\cdot\text{mol}^{-1}$	$N_{\text{B,GPE}}$	$\text{p}K_{\text{a},i}^*$	$\Delta\text{p}K_{\text{a}}(\beta_{\text{GPE}}=1-\alpha_{\text{GPE}})$
14215 ^c	126	6.65 ± 0.07 (62 R ₃ NH ⁺) 9.20 ± 0.05 (64 RNH ₃ ⁺)	$7.25[\exp(-\beta_{\text{GPE}}/7.46)-1]$; $\sim(-0.91 \pm 0.02)\beta_{\text{GPE}}^d$

^a A \equiv RCOO⁻Na⁺; B \equiv R₃N. ^b M_w determined by static light scattering.³⁵ ^c Formula weight. ^d Alternative linear fit.

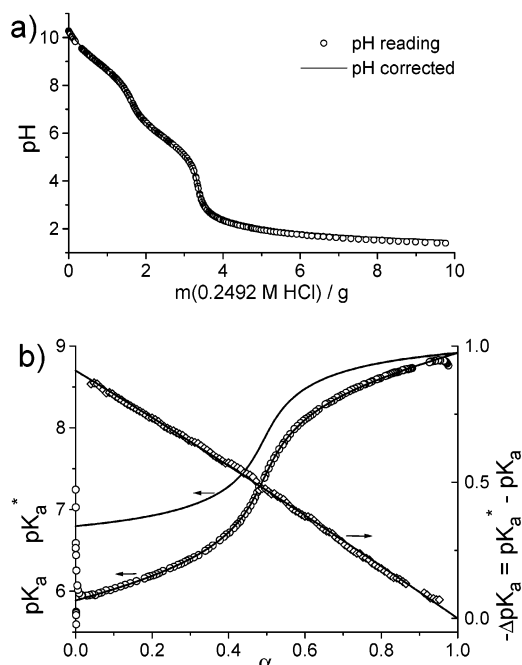


Figure 2. Potentiometric titration of 109 mg of G4-PAMAM in 31.2 cm³ of 0.25 M NaCl with HCl: (a) pH data; (b) extended Hasselbalch (eq 2) transformed data, as a function of the degree of dissociation (α) of G4-PAMAM \cdot 126H⁺. Solid lines show calculated values for the intrinsic and total contribution with the fitted $\text{p}K_{\text{a}}^*$. The right axis shows the nonintrinsic residual contribution and its simultaneous single-exponential fit (eq 23).

compared to the charge density, σ_{HS} , at the surface of a homogeneously charged sphere of radius R_{HS} (eq 8). We look for the radius satisfying $\sigma_{\text{GC}}(r=R_{\text{HS}}) = \sigma_{\text{HS}}(R_{\text{HS}})$, as a function of the degree of dendrimer protonation. At low degrees of charging ($\alpha > 0.7$) the result is $r = R_{\text{HS}} = 1.71$ nm and the curves calculated with this radius are shown as thick lines in Figure 3. At full charging ($\alpha = 0$), the radius required to again satisfy $\sigma_{\text{GC}}(r=R_{\text{HS}}) = \sigma_{\text{HS}}(R_{\text{HS}})$ is 1.77 nm (thin curves in Figure 3). Thus, the dendrimer radius likely increases by about 3.5% upon complete protonation of the primary and tertiary amino groups, and consequently its volume increases by about 11%. Unfortunately, the increase is only significant for a maximum error of 0.02 pH units in the form of an uncompensated (nonlinear) drift of the calibration point of the cell and thus in the $\Delta\text{p}K_{\text{a}}(\alpha)$. Although we found the compensated (linear) part of such a drift to be 0.03 pH units, from the smooth appearance of the curve we can conclude that short-time fluctuations of the calibration point are limited to most probably 0.01 or 0.02 pH units for the cell employed. Consequently, we would need many independent measurements to show the significance of the dendrimer expansion upon charging, but a large expansion (more than 25% in volume) is unlikely even from the single result.

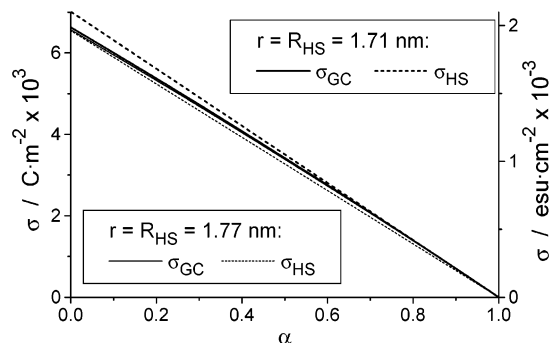


Figure 3. Charge density on G4-PAMAM. Solid lines: σ_{GC} from eq 7 and $\text{p}K_{\text{a}}(\alpha)$ at constant r ; dashed lines: σ_{HS} (eq 8) for spheres with charge $Q_{\text{HS}} = 126(1 - \alpha)e$. The radius $r = R_{\text{HS}} = 1.71$ nm satisfies $\sigma_{\text{GC}} = \sigma_{\text{HS}}$ at low dendrimer charge ($\alpha > 0.8$) whereas $r = R_{\text{HS}} = 1.77$ nm satisfies $\sigma_{\text{GC}}(r) = \sigma_{\text{HS}}(R_{\text{HS}})$ at full protonation ($\alpha = 0$).

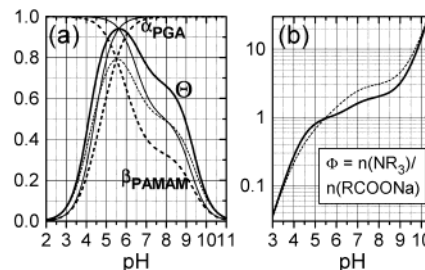


Figure 4. (a) Degree of proton dissociation from PGA (α_{PGA}), of amino group protonation of G4-PAMAM (β_{PAMAM}), and expected degree of ion pairing (Θ) in the neutral PGA_{*m*}-PAMAM_{*n*} complex if there is no specific nor cooperative contribution to it. (b) Stoichiometric ratio (Φ) required for a neutral complex, as function of the pH. Dashed lines are calculated with the apparent (pH dependent) $\text{p}K_{\text{a}}$ of the free, charged polyions, whereas solid lines are calculated with the $\text{p}K_{\text{a}}^*$ for (hypothetically) neutral polyions.

Dissociation Behavior of the IPEC Forming Mixtures. The IPEC dissociation can be calculated from the (charge density-dependent) dissociation constants of the individual polyelectrolytes. Figure 4a shows the calculated degrees of proton dissociation (α) and association (β) and the degree of ion pairing (Θ) for the noncooperative stoichiometric case ($\Phi = 1$), for the extremes of uncharged IPECs and IPECs charged as highly as the noninteracting polyelectrolyte segments of which it is constituted, and with the high-flexibility assumption that all available pairs of oppositely charged groups form ion pairs. In that case, the maximum degree of ion pairing and thus of segment charge neutralization would occur at pH 5.5 where many tertiary amino groups of the dendrimer interior are also protonated, and significant ion pairing would be limited to the pH range between 3 and 10.5. Figure 4b shows the required stoichiometry of a neutral IPEC composed of partially protonated dendrimer and NaPGA under the noncooperative binding conditions: at pH above 5.5 the IPECs will contain excess

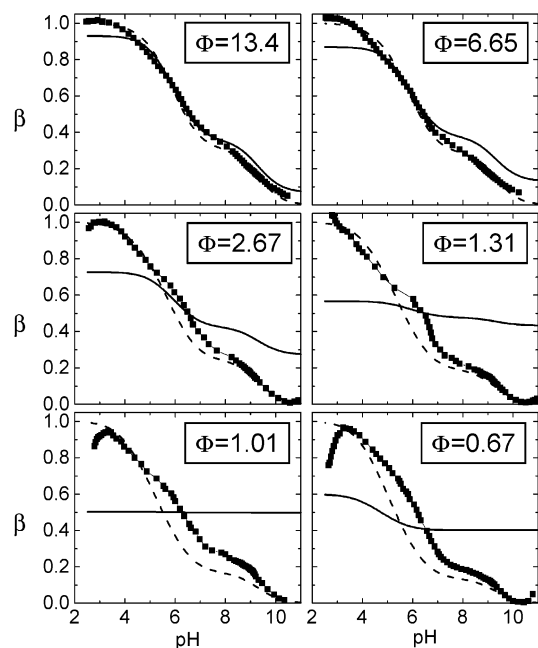


Figure 5. Average degree of protonation of all basic R_3N and $RCOO^-$ groups in PE/IPEC mixtures at different Φ : ■ experimental data from potentiometric titration with slight endpoint adjustments.³⁶ For comparison, modeled β (eq 21) are given for noninteracting ($\Theta = 0$: ---) and fully interacting ($\Theta = 1$: —) PEs, considering noninteracting segments to have the same charge densities as in the individual PEs.

dendrimer, which they would have to release step by step upon protonation.

For six different molar ratios $0.67 \leq \Phi \leq 13.4$ of the dendrimer amino groups to the carboxylic groups of the PGA at constant NaPGA concentration (0.2 g/dm^3), 0.25 N NaOH was added to obtain a pH above 10.5 and the solutions were then titrated with 0.25 N HCl. Generally, stable pH readings could be taken within 1 min after dosage with the titrant. However, very long response times (up to more than 10 min) were observed between pH 6.8 and 4.5 in the cases of $\Phi = 1.31$ and $\Phi = 1.01$, regardless of stirring.

In Figure 5, we show the normalized titration data with slight endpoint adjustments,³⁶ as the overall degree of protonation β vs pH. For comparison we calculated β (using eq 21) for noninteracting ($\Theta = 0$) and fully interacting ($\Theta = 1$) PEs with the $\beta_j(\text{pH})$ of the individual charged PEs, thus considering all noninteracting segments to have the same charge densities as in the individual PEs. At high pH (>10) as well as at low pH (<4) the β values came close to the calculated β for the noninteracting systems, indicating no or weak interaction when one of the PEs is almost uncharged. For $4.5 < \text{pH} < 10$, the observed β is always larger than the expected one for absent interaction. For $\text{pH} > 7$, the experimental data fall between the calculated data for both the limiting Θ , as expected. However, protonation of the dendrimer interior and of the dendrimer-embedded PGA segments apparently already occurs at a pH higher than expected: the crossover is shifted from pH 5.5 (predicted) to ~ 6.5 (experimental), at $\Phi < 2$. This means that the interaction always favors ionization (protonation) of the dendrimer but does not favor ionization of the PGA (dissociation of the carboxylic groups). Instead, the basicity of the carboxylate groups is increased: most probably the activity coefficient for the carboxylate group is increased when it is transferred to the less polar environment of the rather compact IPEC formed when PGA and the dendrimer interiors interpenetrate.

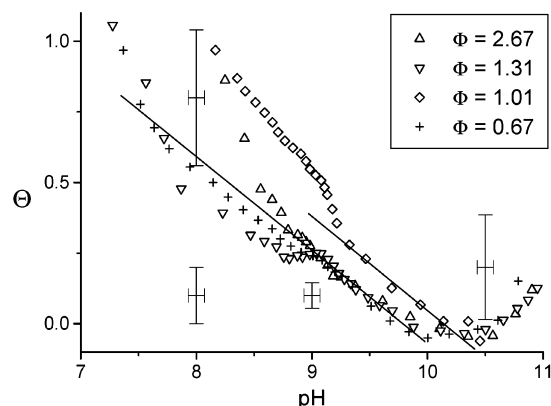


Figure 6. Degree of ion-pair formation Θ , estimated using eq 22, as a function of the pH, at different molar ratios $\Phi = C_0(R_3N)/C_0(RCOONa)$ of the functional groups. The double bars indicate the estimated uncertainty of the absolute values in the corresponding range.

Surprisingly, the shape of the titration curves is very different from the one for the corresponding noninteracting mixture at $\Phi = 1.31$ (1:1 mass ratio) and not at $\Phi = 1.01$, when the polyelectrolytes are present in the stoichiometric ratio required for an entirely ion-paired IPEC. A unique feature of the titration curve at $\Phi = 1.31$ is the high buffering capacity at pH 6.72 which equals, within experimental precision, the intrinsic $\text{p}K_{a,1}^*$ of the tertiary amino groups in the dendrimer core, fitted above as 6.65 ± 0.07 . This suggests that the IPEC formed at $\Phi = 1.31$ has its isoelectric point just at the half-equivalence point of the tertiary amino groups in the dendrimer core, whereas IPECs formed at other Φ are charged at $\text{pH} = \text{p}K_{a,1}^*$.

We have used eq 22 to estimate the conversion ratio, Θ , of pairs of functional groups to ion pairs with released small counterions, in the region of higher pH where the dendrimers become gradually charged. The results are plotted in Figure 6. An approximately balanced stoichiometry was required to observe a significant deviation of the β of the interacting system from the corresponding β of the noninteracting system. One observes that ion pairing starts at $\text{pH} \sim 10.5$; an error of ± 1 pH unit has to be considered for this onset because of the possibly improper titration endpoint adjustment. The initial increase in Θ with decreasing pH is approximately linear with a Φ -independent slope $d\Theta/d\text{pH} = -0.33 \pm 0.05$, and the error of the slope is only slightly affected by the possibly improper endpoint adjustment. After Θ has increased to values between 0.25 and 0.5, $-d\Theta/d\text{pH}$ tends to become much stronger, and Θ most likely approaches 1 (quantitative ion pairing), although this cannot be stated from our data with any unambiguity.

Complexation upon Dendrimer Protonation: Turbidity Measurements. At each titration step of the potentiometric titration, the turbidity has been measured at $\lambda_0 = 355 \text{ nm}$. At this short wavelength, the turbidity was most sensitive to the initial increase in the weight-average molecular weight, M_w , due to IPEC formation, as shown in Figure 7a. The turbidity at pH 11 to ~ 8.8 , where the turbidity is $\propto M_w$, is increased with decreasing pH in three steps. Starting at a pH between 11 and 10.5 (onset 1 in Figure 7b), the increase is linear with the decreasing pH down to a pH of 9.4 ± 0.1 where τ attains values around 0.1 (τ at onset 2 in Figure 7c). The second step in the turbidity and corresponding M_w increase is observed in the very narrow pH range between 9.4 ± 0.1 (onset 2) and 9.17 ± 0.05 . In that process, however, the τ increase seems to be again linear with the pH with a significantly increased slope of $-d\tau/d\text{pH}$. At the “end” of the second step (at onset 3) τ attains values between 0.2 and 0.4, more than twice as high as at onset 2.

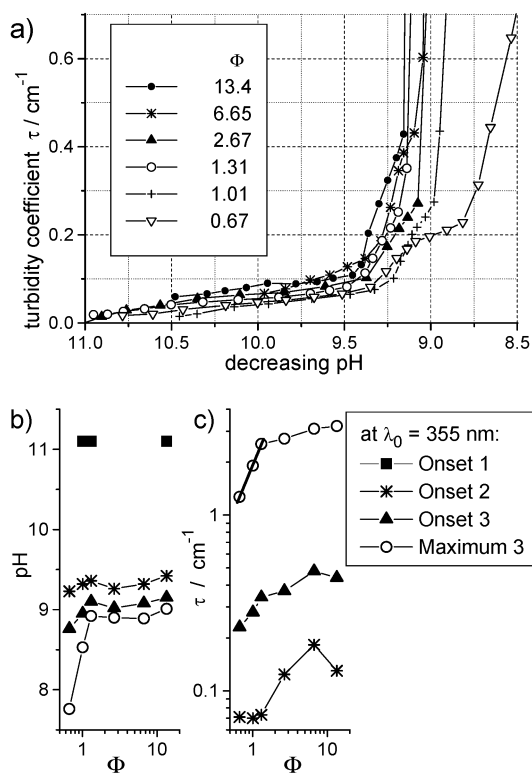


Figure 7. (a) Turbidimetric titration of 0.2 g/L NaPGA and 0.2(Φ /1.33) mg/cm³ G4-PAMAM with HCl, at wavelength $\lambda_0 = 355 \text{ nm}$. (b) pH and (c) corresponding turbidities, at onsets of the first changes upon pH decrease and at the turbidity maximum.

When the pH decreases to below 9.17 (onset 3), in all mixtures with excess of the dendrimer amino groups over carboxylic groups ($\Phi > 1$) the turbidity increases by about 1 order of magnitude in a pH range as narrow as 0.2. It should be noted that at higher HPE concentrations (1 mg/cm³), macroscopic phase separation (coacervation) was observed at this pH.

In the case of excess HPE ($\Phi = 0.67$), the last aggregation process is shifted to considerably lower pH values and becomes much less abrupt, as can be seen from the increased pH range between onset 3 and maximum 3 in Figure 7b.

Discussion

Dissociation of Poly(L-glutamic acid). Our fitting of the titration curve $pK_a(\alpha)$ to three linear regimes is not in accord with the expected behavior of a thin charged cylinder. To show this, we have included in Figure 2 the best fits with the prediction from the CC theory for the noncondensing regime (eq 11). Obviously, these curves do not correctly describe the behavior at a high degree of dissociation, unless one admits a gradual decrease in the average distance between functional groups, b_1 , from 0.77 to 0.66 nm when α increases above the helix-coil transition from 0.73 to 1, or one assumes an unreasonably low intrinsic $pK_{a,1}^* \approx 3.1$ (fit not shown), combined with $b_1 \approx 0.4$. For the low α , an effective distance of $b_1 = 0.77 \pm 0.03 \text{ nm}$ between ionizable groups fits the data best, especially in the transition plateau, but not accurately in the measured part of the α -helical regime. The discrepancy is obviously due to the large distance between the polymer rod axis and the ionic sites at the ends of the side chains (0.5 nm in the coil, 0.7 nm in the α -helix), which make the electrostatic structure a fuzzy, nonuniformly charged cylinder rather than a thin one, when comparing sizes to either the Bjerrum length or the Debye-Hückel screening length. Although the distance b_1

between functional groups along the rod axis is reported to be shorter than both l_B and κ^{-1} ($b_1 = 0.36$ and 0.15 nm in the coil and α -helical conformations, respectively), the effective distance of $b_{\text{eff}} \approx 0.7 \text{ nm}$ between neighboring charges is obviously just close to the Bjerrum length.

Dissociation of G4-PAMAM Dendrimer. The obtained value of 9.2 for the intrinsic $pK_{a,2}^*$ reflects a much lower basicity of the primary amino groups in the PAMAM dendrimer than in ethylenediamine ($pK_a = 9.9$). Tomalia et al.²³ studied briefly the protonation of G0–G3 PAMAM-NH₂ dendrimers with ammonia and ethylenediamine cores and found a similar polyelectrolyte behavior for these dendrimers with two distinguishable equivalent points; the more acidic one corresponding to the tertiary amines and the more basic one to the peripheral primary amines. The pK_a^* values in the present work compare well with those found by Barbucci et al.²⁴ for linear poly(amido amine) where the tertiary amino groups in the vicinity of the amide group exhibit a considerably lower basicity ($pK_{a,1}^*$ typically around 6.5 ± 1.5) than the tertiary amino groups of the more peripheral side chains ($pK_{a,2}^*$ typically around 9.1 ± 0.4). Ottaviani et al.²⁵ calculated a distribution function of $pK_a(\text{pH})$ from titration curves of G3 and G5 PAMAM-NH₂ dendrimers with the amine core and attributed $pK_a(\text{pH})$ between 8.5 and 13.2 to protonated peripheral primary amines, $pK_a(\text{pH})$ between 7.6 and 5.7 to protonated NR₃ groups in the outer shell, and $pK_a(\text{pH})$ between 5.6 and 3.4 to those in the interior shells; the spectrum of pK_a shifts to lower pK_a upon increase of dendrimer generation.

When our $pK_{a,2}^*$ and $pK_{a,1}^*$ (9.2 and 6.65) results for the primary and tertiary amino groups are compared, respectively, with those reported for poly(propylenimine) dendrimers in water (9.75 and 6.1),²⁷ we find the $pK_{a,2}^*$ of the PAMAM dendrimer to be 0.55 lower than the corresponding $pK_{a,2}^*$ of the PPI dendrimer, and the $pK_{a,1}^*$ of the tertiary amino groups of the G4-PAMAM to be higher by the same difference (0.55) than the corresponding $pK_{a,1}^*$ of the G3-PPI dendrimer. The obvious leveling of the basicity in the set of quasi-sites³⁴ of the PAMAM dendrimer could be due to some sort of coupling between the different amino groups, e.g., through intramolecular hydrogen-bond formation with the amide groups²⁴ which are not present in the PPI dendrimers.

The found distance, r , of the Helmholtz plane from the center of the G4-PAMAM dendrimer ($r = 1.71 \text{ nm}$, increasing to 1.77 nm on full charging) compares well with the radius of gyration, R_g , of the dendrimer, obtained from SAXS measurement of a 1% aqueous solution as $R_g = 1.78 \text{ nm}$.³⁷ The even smaller value indicates that many of the charged amino termini are folded inward instead of forming a shell at the periphery and that the electrostatic repulsion is far weaker than the steric energy associated with a stretched conformation of the dendrons.

The calculated increase in the dendrimer volume by about 11% upon complete protonation of its 126 amino groups agrees qualitatively with AFM measurements of G6–G9 PAMAM dendrimers where an increase in volume of up to 33% was observed on protonation.³⁸ On the other hand, Nisato et al.³⁹ found from SANS that the sterically more constrained G8-PAMAM dendrimer expands only less than 1% in diameter, if at all. A significant expansion (up to 70% in diameter) upon charging of some model dendrimers of lower generations is predicted by simulations,⁴⁰ and conformational changes have been proposed (expulsion of backfolded charged end groups to the periphery when the interior becomes protonated at lower pH⁴¹).

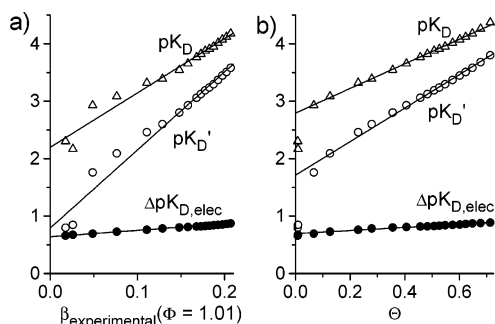


Figure 8. pK_D' and pK_D for an ion-pair separation in an IPEC, calculated from $\Theta(\text{pH}, \Phi=1.01)$ with eq 19. The linear fits are $pK_D' = (1.21 \pm 0.03) + (11.1 \pm 0.2)\beta$, $pK_D = (1.71 \pm 0.03) + (2.92 \pm 0.07)\Theta$ and $pK_D = (2.5 \pm 0.1) + (7.6 \pm 0.4)\beta$, $pK_D = (2.79 \pm 0.02) + (2.14 \pm 0.03)\Theta$, respectively. For comparison, with solid symbols: calculated $\Delta pK_{D,\text{elec}}$ for PE mixture at $\Phi = 1.01$, using data from Figure 4, with the linear fits $\Delta pK_{D,\text{elec}} = 0.64 + 1.13\beta$ and $\Delta pK_{D,\text{elec}} = 0.70 + 0.27\Theta$, respectively.

Dissociation of the IPEC Forming Mixtures. To see the extent of the cooperativity of the ion-pair formation in the IPECs, we combine the $\Theta(\text{pH})$ data of Figure 6 with the $\beta(\text{pH})$ data of Figure 5 to get the function $pK_D(\beta)$ (using eqs 18 and 19). Our results for the $\Phi = 1.01$ mixture (Figure 8) show an almost linear increase of the pK_D with the initially increasing β and, even better, with the increasing Θ upon dendrimer protonation. In other words, the dissociation constant of a certain ion pair decreases when the total number of ion pairs in the IPEC is increased, and thus ion pairing of the remaining unpaired segments of an existing IPEC is favored against ion pairing to form a new IPEC. The cooperativity in the ion pairing should mainly be due to the “pinning” of the mutual steric orientation of the interacting charge patches. On an ion-pair dissociation that is not the first or second one fixing an *individual* GPE to the HPE, the dissociated groups remain close to one another and the probability of a reencounter is highly increased, whereas the frequency of ion-pair dissociation should be insensitive to the steric factor.

One part of the ΔpK_D , the contribution $\Delta pK_{D,\text{elec}}$, is due to the extra work, $\Delta G_{D,\text{elec}}$, required to charge-separate the ion pair against the actual surface potentials, ψ_0 , of both interacting PEs. This work is $\Delta G_{D,\text{elec}} = F|\psi_{0,\text{GPE}} - \psi_{0,\text{HPE}}|$. $\Delta pK_{D,\text{elec}}$ thus equals the sum of the absolute values of the ΔpK_a : $\Delta pK_{D,\text{elec}}(\beta) = |\Delta pK_{a,\text{GPE}} - \Delta pK_{a,\text{HPE}}|\beta$. The increase in $\Delta pK_{D,\text{elec}}$ with β or Θ (see Figure 8) is only a minor contribution to $dpK_D/d\Theta$ when the cooperativity of the ion-pair formation is large.

Quantitatively, the fitted slope $dpK_D/d\Theta = 2.14 \pm 0.03$ indicates that in the range $0.03 < \Theta < 0.7$ the stability of an ion pair in the IPEC is proportional to the number of ion pairs contributed by one dendrimer GPE, because $126 = 10^{2.10}$ ion pairs would be contributed by each GPE at $\Theta = 1$. Generally, one might expect a slope $dpK_D/d\Theta = \log(z_{\text{GPE}} \text{ at } \Theta = \Phi = 1) + d\Delta pK_{D,\text{elec}}/d\Theta$. However, for the first bound sites, at $\Theta < 0.03$, the stability of the ion pair is lower (here about 5-fold), because the mutual orientation of HPE and GPE is not yet fixed.

So far we cannot check the general validity of the above expression for the slope $dpK_D/d\Theta$. Although there are a lot of data that probe the different titration behaviors of isolated PEs and their stoichiometric IPECs,^{9,16} the function $pK_D(\Theta)$ has apparently never been reported. We compare instead our $\Theta(\text{pH})$ data (Figure 5) with those for the titration of IPECs of poly(propyleneimine) dendrimers (PPI) and poly(acrylic acid) (PAA) reported by Kabanov et al.¹⁶ Their data also show an

initially linear increase of Θ with decreasing pH, with a slope $d\Theta/d\text{pH} = -0.44$ independent of the dendrimer generation. Our finding for the slope is $d\Theta/d\text{pH} = -0.33$, independent of the Φ . The lower absolute value may be due to a smaller linear charge density of the HPE (PGA instead of PAA) and thus a lower pK_D at $\Theta \rightarrow 0$, but a quantitative comparison is difficult because Θ depends nonlinearly on the pK_a of the PEs and the pH, in addition to the pK_D .

However, neither cooperativity nor anticooperativity of the collective binding of several *different* guests to one HPE was found for the interaction between a linear HPE and charged micelles as guest colloids;⁴² in that case, the binding was measured by ultrafiltration and the binding isotherm fitted by a Hill plot.

Complexation upon Dendrimer Protonation. The onset of IPEC formation upon lowering the pH to below some critical value, $\text{pH}(\sigma_C)$, has been detected by the increase in the degree of ion-pair formation, Θ , from zero, linearly with the decrease in the pH, and from the increase in the turbidity, τ , which is proportional to the weight-average molecular weight, M_w . The turbidity starts to increase at $\text{pH}(\sigma_C) = 11.0 \pm 0.2$, independent of the GPE excess. Ion pairing starts at an observed $\text{pH}(\sigma_C) = 10.5 \pm 0.5$, which is not significantly different. If the two $\text{pH}(\sigma_C)$ values were not identical, one would have to conclude a mere correlation of the macroionic clouds of the oppositely charged PEs before ion pairing starts at a higher dendrimer charge. The macroionic cloud interaction would have to be rather effective; otherwise it could not change the structure factor to such an extent that it would have the measured effect on the turbidity. The more likely case is that the two $\text{pH}(\sigma_C)$ values are identical. Then, above the critical charge density, σ_C , macroions bind to the HPE through ion pair formation, so that the M_w ($\propto \tau$) increases together with Θ . Another argument for this scenario is that there is obviously no sudden break in the turbidity evolution close to pH 10.5 or 10. Both Θ and τ increase linearly with decreasing pH in a range as wide as 1 pH unit. We conclude that M_w ($\propto \tau$) increases linearly with Θ for small charge densities just above σ_C and that the initial increase in Θ is due to an almost proportional increase in the total number of HPE-bound GPEs, in accord with the previously examined cooperativity.

We will now analyze the electrostatic interactions at the breaks in the turbidity increase from Figure 6. At $\text{pH}(\sigma_C) = 11$, it can be calculated from eq 2 that $\beta_{\text{GPE}} = 0.008$, corresponding to just one positive elementary charge on the dendrimer on average, and thus to a very inhomogeneous charge density. At pH 10.5 we would have $\beta_{\text{GPE}} = 0.024$ and thus three positive charges (in excess to the ion-paired ones), which should be screened from each other, considering the large diameter of the dendrimer (3.5 nm) in comparison with the Debye–Hückel screening length (0.61 nm). To find the minimum dendrimer charge at which it will be felt as a polyion with correlated charges rather than one with screened isolated charges, we estimate the average distance between charges on the dendrimer. By dividing the dendrimer surface (taken as a sphere with $R_{\text{HS}} = 1.75$ nm) by the number z_{GPE} of elementary charges, e , which it carries on average at a given pH, we calculate the radius, $r_e = R_{\text{HS}}/(4z_{\text{GPE}}/3)^{1/2}$, of a circular plane area occupied by any of these charges and show it in Table 2 at the pH of the break points in the turbidity behavior, for the extreme cases of zero charge density and potential ($\psi_{\text{HS}} = 0$, due to 100% charge compensation in the Helmholtz plane, e.g., by ion-pair formation) and of zero counterion adsorption ($\psi_{\text{HS}} = \psi_0$), respectively. It turns out that the first break in the turbidity evolution (onset 2) occurs when, at pH 9.4, $r_e(\psi_{\text{HS}}=0)$ becomes equal to the

TABLE 2: Calculated Number of Protonated Amino Groups per Dendrimer and Charge Distances r_c on the Dendrimer Surface, at the “Critical” pH Where IPEC Formation with PGA and IPEC Aggregation Starts or Goes to Maximum

behavior (Figure 6)	pH	if effective $\psi_0 = \Delta pK_{a,GPE} = 0$			if effective $\psi_0 = \psi_{HS}$		
		β_{GPE}	Z_{GPE}	$r_c/nm^{a,b}$	β_{GPE}	Z_{GPE}	$r_c/nm^{a,b}$
onset 1	11.0	0.008	1.0	3.5	0.008	1.0	3.5
	10.5	0.024	3.0	2.0	0.023	2.9	2.1
onset 2	9.40	0.196	25	0.70	0.149	19	0.80
onset 3	9.17	0.264	33	0.61	0.191	24	0.71
maximum 3 (at various Φ)	8.95	0.327	41	0.55	0.227	29	0.66
	8.76	0.375	47	0.51	0.255	32	0.62
	7.91	0.500	63	0.44	0.329	41	0.54
	7.76	0.515	65	0.44	0.337	42	0.54

^a Calculated with $R_{HS} = 1.75$ nm; ^b Compare with $l_B = 0.714$ nm, $\kappa^{-1} = 0.608$ nm, and $b_{HPE,eff} \sim 0.7$ nm.

Bjerrum length, l_B , or to the effective charge distance, $b_{HPE,eff}$, on the PGA fuzzy cylinder. At the second transition (onset 3, at pH 9.17), the estimated $r_c(\psi_{HS} = 0)$ becomes equal to κ^{-1} . The significance of the latter correlation could, however, be easily checked by varying the ionic strength, as has been done in a large number of other works⁹ with the result that $\sigma_C' \propto \kappa$. This supports the involvement of the Debye screening length in the first *substantial* turbidity increase (the first measurable in practice at high wavelengths), usually taken as the critical charge density for IPEC formation and here denoted σ_C' . Usually, only this break in the turbidity evolution with the pH was observed, e.g., for the interaction between strong PEs. Instead, our results support the idea that IPEC formation begins in a mass-action process⁴² with no relation to a critical charge density, before it turns into the surface-interactive aggregation process associated with the considerable turbidity increase (at onset 2), at least in the case of the interaction of the small PEs to be considered here. The latter aggregation process finally leads to phase separation at another break at onset 3, in our case coacervation, at higher PE concentrations. At even higher degrees of protonation, IPECs become overcharged and again less compact because of swelling induced by the electrostatic repulsion of their charged segments. Overcharging is limited, and thus fewer GPEs can bind to one HPE at high β , which is especially significant at high dendrimer excess. This leads to the observed decrease in M_w of the IPEC (and in τ) upon strong protonation in the case of $\Phi > 1$. Some further details of the structural evolution of the IPECs will be examined and presented in a forthcoming paper.

Finally, we now discuss our finding from Figure 6 that a degree of conversion to ion pairs considerably larger than 0.5 was usually achieved at pH ~ 8 , well above the intrinsic $pK_{a,1}^*$ (6.65) of the tertiary amino groups in the dendrimer interior. This is clear evidence that these amino groups become protonated to a considerable extent only to participate in ion pairs with the carboxylic groups of the HPE because of a high pK_D resulting from the cooperative ion pairing (see above). To achieve this coupling, either mutual interpenetration of the HPE and the dendrimer is required, which is sterically pretentious but may yield close ion pairs, or the correlation of the ionic sites is by distant ion pairs, which are nevertheless correlated so much (e.g., by constraints due to covalent linkage to the slowly fluctuating “cage” made by neighboring close ion pairs) that their counterions may escape more frequently from the ionic cloud than habitual for independent macroions. The extent of true interpenetration thus remains an open question. The steric energy associated with this likely needs to be compensated not only by the entropy increase of the released counterions but also by the enthalpically favorable interaction between the interpenetrating segments, for example, additional hydrogen

bonds between the amide groups in the polypeptide backbone and those of the dendrimer branches.

Kabanov et al.¹⁶ found that the carboxylate of poly(acrylic acid) binds equally to primary and tertiary ammonium groups (in the dendrimer interior), whereas sulfonate groups attached to a polystyrene backbone bind strongly to only the primary ammonium terminal groups of a poly(propylenimine) dendrimer. A strong turbidity increase was observed by these authors when the degree of ion pair formation, Θ , exceeded 0.52, at $\Phi = 1$. This compares with our data, where at $\Phi = 1.01$ and $\Theta \sim 0.51$ the corresponding pH (9.07; Figure 5) was only 0.12 units lower than the pH at the onset of the strong turbidity increase leading to the τ maximum (onset 3, Figure 6). The turbidity increase is probably due to a secondary aggregation of IPECs, which would explain the strong M_w increase of the IPEC clusters (onset 3). At the maximum turbidity, the complexes would be electro-neutral and the aggregates could assume a more compact structure, which then swells again as the IPECs become overcharged, and finally lose dendrimer macroions to limit the overcharging at higher degrees of protonation, letting the M_w decrease.

Conclusions

The binding of the protonated dendrimer G4-PAMAM as a guest polyelectrolyte (GPE) to the anionic homopolyelectrolyte NaPGA has been investigated by potentiometric titration in 0.25 M aqueous NaCl solution. The polyelectrolyte behavior of the individual polyelectrolytes (PEs) was studied first. The results have been used to calculate the polyelectrolyte behaviors for hypothetically noninteracting mixtures of the PEs at different stoichiometric ratios, Φ , of the dendrimer’s 126 chargeable amino groups to the ≈ 300 carboxylate groups of the NaPGA. The behaviors were compared with the experimental polyelectrolyte behaviors of the corresponding interacting mixtures. From the difference in the overall degree of protonation, β , at a given pH and Φ , the degree of conversion, $\Theta(pH)$, of pairs of ionizable groups to ion pairs with released counterions was calculated and related to the thermodynamic dissociation constant, K_D , of an average ion pair in the interpolyelectrolyte complex (IPEC).

Upon dendrimer protonation and charging below pH 11, ion pair formation starts when the pH is lowered to about 10.5. The degree of ion-pair formation, Θ , increases linearly with decreasing pH down to values of about 0.25, where the slope of this increase is virtually independent of the stoichiometry, Φ , and the onset is almost identical with the onset of a slight linear turbidity increase to be taken as the onset of IPEC formation. At even lower pH, Θ certainly attains values above 0.5, indicating that at least some of the protonated tertiary amino-groups in the inner shells of the dendrimer are involved in direct ion pairing with carboxylate groups of the host polyelectrolyte (HPE).

The pK_D value increases linearly with the initially increasing Θ upon protonation of the PE mixture. The slope $\langle dpK_D/d\Theta \rangle_{\Theta < 0.3}$ is found to be 8-fold higher than expected due to a change in $pK_{D,elec}$ corresponding to the β -dependent work for charge separation of a single ion pair, indicating a highly cooperative ion pair formation between those sites belonging to a single HPE/GPE pair.

An unexpected high buffering capacity at the pH equal to the intrinsic $pK_{a,1}^*$ of the tertiary amines in the dendrimer interior has been found in the unstoichiometric complexes with a 1.31-fold excess of the amino groups on the dendrimer to the number of carboxylic groups on the HPE, indicating that the excess isolated sites in the dendrimer interiors of the IPEC behave as in an essentially screened environment and thus the IPEC is an electroneutral colloid at this pH, whereas at other Φ the isoelectric points of the IPEC and the $pK_{a,1}^*$ are different.

Acknowledgment. This work was financially supported by the Mitsubishi Foundation.

References and Notes

- (1) Michaels, A. S. *Ind. Eng. Chem.* **1965**, *57*, 32.
- (2) Rigsbee, D. R.; Dubin, P. L. *Langmuir* **1996**, *12*, 1928–9.
- (3) Simmons, C.; Webber, S. E.; Zhulina, E. B. *Macromolecules* **2001**, *34*, 5053–66.
- (4) Kabanov, V. A. In *Macromolecular Complexes in Chemistry and Biology*; Dubin, P., Bock, J., Davies, R. M., Schulz, D. N., Thies, C., Eds.; Springer: Berlin, 1994; Chapter 10, pp 151–74.
- (5) Koetz, J.; Koepke, H.; Schmidt-Naake, G.; Zarras, P.; Vogl, O. *Polymer* **1996**, *37*, 2775–81.
- (6) Mizusaki, M.; Morishima, Y.; Yoshida, K.; Dubin, P. L. *Langmuir* **1997**, *13*, 6941–6.
- (7) Kawamoto, T.; Morishima, Y. *Langmuir* **1998**, *14*, 6669–75.
- (8) Miura, N.; Dubin, P. L.; Moorefield, C. N.; Newkome, G. R. *Langmuir* **1999**, *15*, 4245–50.
- (9) Zhang, H.; Dubin, P. L.; Ray, J.; Manning, G. S.; Moorefield, C. N.; Newkome, G. R. *J. Phys. Chem. B* **1999**, *103*, 2347–54.
- (10) Odijk, T. *Langmuir* **1991**, *7*, 1.
- (11) Mizusaki, M.; Morishima, Y.; Dubin, P. L. *J. Phys. Chem. B* **1998**, *102*, 1908–15.
- (12) Xia, J.; Dubin, P. L. In *Macromolecular Complexes in Chemistry and Biology*; Dubin, P., Bock, J., Davies, R. M., Schulz, D. N., Thies, C., Eds.; Springer: Berlin, 1994; Chapter 15, pp 247–71.
- (13) Park, J. M.; Muhoherac, B. B.; Dubin, P. L.; Xia, J. *Macromolecules* **1992**, *25*, 290–5.
- (14) Mansfield, M. L. *Macromolecules* **2000**, *33*, 8043–9.
- (15) Welch, P.; Muthukumar, M. *Macromolecules* **2000**, *33*, 6159–67.
- (16) Kabanov, V. A.; Zezin, A. B.; Rogacheva, V. B.; Gulyaeva, Zh. G.; Zansochova, M. F.; Joosten, J. G. H.; Brackman, J. *Macromolecules* **1999**, *32*, 1904–9.
- (17) Kabanov, V. A.; Sergeev, V. G.; Pyshkina, O. A.; Zinchenko, A. A.; Zezin, A. B.; Joosten, J. G. H.; Brackman, J.; Yoshikawa, K. *Macromolecules* **2000**, *33*, 9587–93.
- (18) Brown, M. D.; Schätzlein, A. G.; Uchegbu, I. F. *Int. J. Pharm.* **2001**, *229*, 1–21.
- (19) Gebhart, C. L.; Kabanov, A. V. *J. Controlled Relat.* **2001**, *73*, 401–16.
- (20) Pillai, O.; Panchagnula, R. *Curr. Op. Chem. Biol.* **2001**, *5*, 447–51.
- (21) Ottaviani, M. F.; Sacchi, B.; Turro, N. J.; Chen, W.; Jockusch, S.; Tomalia, D. A. *Macromolecules* **1999**, *32*, 2275–82.
- (22) Nagasawa, M.; Holtzer, A. *J. Am. Chem. Soc.* **1964**, *86*, 538.
- (23) Tomalia, D. A.; Baker, H.; Dewald, J.; Hall, M.; Kallos, G.; Martin, S.; Roeck, J.; Ryder, J.; Smith, P. *Polym. J. (Tokyo)* **1985**, *17*, 117–132.
- (24) Tomalia, D. A.; Naylor, A. M.; Goddard, W. A. *Angew. Chem., Int. Ed. Engl.* **1990**, *29*, 138–75.
- (25) Barbucci, R.; Casolaro, M.; Ferruti, P.; Barone, V.; Lelj, F.; Oliva, L. *Macromolecules* **1981**, *14*, 1203–9.
- (26) Ottaviani, F.; Montalti, F.; Romanelli, M.; Turro, N. J.; Tomalia, D. A. *J. Phys. Chem.* **1996**, *100*, 11033–11024.
- (27) Nishio, T. *Biophys. Chem.* **1998**, *71*, 173–84.
- (28) Kabanov, V. A.; Zezin, A. B.; Rogacheva, V. B.; Gulyaeva, Zh. G.; Zansochova, M. F.; Joosten, J. G. H.; Brackman, J. *Macromolecules* **1998**, *31*, 5142–4.
- (29) Davies, C. W. *J. Chem. Soc.* **1938**, 2093–8.
- (30) Robinson, R. A.; Stokes, R. H. *Electrolyte Solutions*, 2nd ed.; Butterworth: London, 1959; pp 230–6.
- (31) Loeb, A. L.; Overbeek, J. Th. G.; Wiersema, P. H. *The Electrical Double Layer around a Spherical Particle*; MIT Press: Cambridge, U.K., 1961.
- (32) Manning, G. S. *J. Phys. Chem.* **1984**, *88*, 6654.
- (33) Porasso, R. D.; Benegas, J. C.; van den Hoop, M. A. G. T.; Paoletti, S. *Biophys. Chem.* **2000**, *86*, 59–69.
- (34) Cesàro, A.; Delben, F.; Flaibani, A.; Paoletti, S. *Carbohydr. Res.* **1987**, *161*, 355.
- (35) Onufriev, A.; Case, D. A.; Ullmann, G. M. *Biochemistry* **2001**, *40*, 3413–9.
- (36) Imae, T.; Miura, A. *J. Phys. Chem. B* **2003**, *107*, 8088–92.
- (37) The adjustment is done by introducing a constant offset ΔpH to match the drifted pH; it is added to all measured pH values of a titration and chosen to yield the following conditions for $\beta(V_{HCl}, pH + \Delta pH)$: at highest pH values (> 12), β must never become negative but approach zero. This condition is somewhat problematic to be really measured, because a small error in pH corresponds to a considerable error in the estimated concentration $C(OH^-)$ and thus to a large error in β . At low pH values, $\beta(V_{HCl}, pH + \Delta pH)$ becomes also very sensitive to changes in the ΔpH fitting parameter. ΔpH should be additionally constrained to match the condition that β increases monotonically, when pH decreases. Further, β should keep inside the range of its definition between 0 and 1. On the other hand, in the range of generally small $C(H^+)$ and $C(OH^-)$ compared to the concentration of polyelectrolyte basic groups, thus in the range $5 < pH < 9$, $(\partial^2\beta/\partial pH^2)_V$ is practically insensitive to errors in the pH, whereas $(\partial\beta/\partial pH)_V \propto \beta_{max} - \beta_{min}$, the total amplitude of the $\beta(V_{HCl}, pH + \Delta pH)$ function. In that range, a change of the ΔpH parameter results in both a vertical shift and a vertical expansion or compression of the $\beta(pH)$ functions displayed in Figure 5, but the shape of the curve, that is the function $(\beta(pH) - \beta_{min})/(\beta_{max} - \beta_{min})$, does not change significantly with the choice of ΔpH except for the plateau regions at lowest and highest pH. A plateau value $\beta_{max} = 1$ may only be reached if all ion pairs involving $R-COO^-$ are broken up by a proton activity high enough to protonate the uncharged $R-COO^- \cdot HNR'_3^+$ sites.
- (38) Prosa, T. J.; Bauer, B. J.; Amis, E. J. *Macromolecules* **2001**, *34*, 4897–906.
- (39) Betley, T. A.; Banaszak Holl, M. M.; Orr, B. G.; Swanson, D. R.; Tomalia, D. A.; Baker, J. R., Jr. *Langmuir* **2001**, *17*, 2768–73.
- (40) Nisato, G.; Ivkov, R.; Amis, E. J. *Macromolecules* **2000**, *33*, 4172–6.
- (41) Welch, P.; Muthukumar, M. *Macromolecules* **1998**, *31*, 5892–7.
- (42) Chen, W.; Tomalia, D. A.; Thomas, J. L. *Macromolecules* **2000**, *33*, 6169–72.
- (43) Feng, X.; Dubin, P. L. *Langmuir* **2002**, *18*, 2032–5.